

- R. Strong, Jr., D. Simberloff, L. G. Abele, A. B. Thistle, Eds. (Princeton Univ. Press, Princeton, NJ, 1984), pp. 151–180; J. Roughgarden, Y. Iwasa, C. Baxter, *Ecology* 66, 54 (1985); J. H. Connell, *J. Exp. Mar. Biol. Ecol.* 93, 11 (1985).
3. S. D. Gaines and J. Roughgarden, *Proc. Natl. Acad. Sci. U.S.A.* 82, 3707 (1985); S. D. Gaines *et al.*, *Oecologia (Berlin)* 67, 267 (1985).
  4. San Francisco, California, to Baja California, Mexico, and Peru to Tierra del Fuego. M. S. Foster and D. R. Schiel, "The ecology of giant kelp forests in California: A community profile" [*U.S. Fish Wildl. Serv. Biol. Rep.* 85(7.2) (1985)]; P. K. Dayton, *Annu. Rev. Ecol. Syst.* 16, 215 (1985).
  5. P. K. Dayton *et al.*, *Ecol. Monogr.* 54, 253 (1984).
  6. L. F. Lowry and J. S. Pearce, *Mar. Biol.* 23, 213 (1973); J. A. Estes and J. F. Palmisano, *Science* 185, 1058 (1974); D. O. Duggins, *Ecology* 61, 447 (1980).
  7. P. K. Dayton and M. J. Tegner, *Science* 224, 283 (1984).
  8. G. A. Jackson and C. D. Winant, *Cont. Shelf Res.* 2, 75 (1983); G. A. Jackson, *J. Phys. Oceanogr.* 14, 1300 (1984).
  9. G. A. Jackson, in *Biochemical and Photosynthetic Aspects of Energy Production*, A. San Pietro, Ed. (Academic Press, New York, 1980), pp. 31–80.
  10. B. B. Bernstein and N. Jung, *Ecol. Monogr.* 49, 335 (1979).
  11. R. N. Bray, *Fish. Bull. (Dublin)* 78, 829 (1980).
  12. Samples (200 liters each) were taken from April through June. Thereafter, samples were increased to 400 liters because of low abundances in some taxa.
  13. R. K. Grosberg, *Ecology* 63, 894 (1982); S. D. Gaines and J. Roughgarden, unpublished data.
  14. Late stage II nauplii eventually exhibit weak negative phototaxis.
  15. S. D. Gaines and J. Roughgarden, unpublished data.
  16. Early stage barnacle nauplii may be the exception because laboratory studies suggest nauplii are more readily eaten by several invertebrates resident in the kelp canopy (for example, caprellid amphipods, mysids). Their concentrations may also be affected by changes in phototaxis with development (14).
  17. D. J. Miller and J. J. Geibel, *Calif. Fish Game Bull.* 158 (1973).
  18. T. W. Anderson, thesis, California State University, Fresno (1983). *Sebastes atrovirens*, the kelp rockfish, is a noteworthy exception that reaches peak juvenile abundance in autumn. It was relatively rare throughout the study.
  19. M. M. Singer, thesis, San Jose State University, San Jose, California (1982); S. D. Gaines and J. Roughgarden, unpublished data.
  20. The rockfish are concentrated primarily at the perimeter of the bed (11), and yearly variation in fish density is probably more important than yearly variation in kelp canopy area per se. A more definitive test awaits years in which rockfish recruitment success is decoupled from yearly fluctuations in kelp canopy area.
  21. The cause of the relation is under further study. It is unlikely, however, that the observed variation in rockfish density was a direct response to changes in kelp bed area since parallel annual fluctuations were seen throughout the central California coast including rockfish species that do not recruit to kelp beds (unpublished data from E. Hobson). Moreover, preliminary data from 1986 show that rockfish recruitment rates are low despite a large kelp canopy comparable to that of 1985.
  22. The error bars pertain to observation error inherent in measuring recruitment rates from several quadrats; the error does not represent the sample variance in recruitment from different years in which the canopy area was the same. Therefore, the differences in confidence interval size are largely irrelevant to the assumption of homoscedasticity.
  23. Unpublished data from E. Hobson for the Mendocino coast. Less extensive records and qualitative reports from the California Department of Fish and Game suggest comparable patterns for Monterey Bay. Counts are number of fish seen per minute of water column observation time during the peak abundance periods of July and August. Totals of 45, 67, and 277 minutes of observation are included for 1983, 1984, and 1985, respectively. This density estimate probably has a conservative bias at high fish densities.
  24. We thank C. Baxter, S. Brown, M. Denny, and T. Hahn for comments and field assistance, the Department of Energy (EV10108) for primary financial support, and the National Science Foundation (OCE 85-14755) for supplemental funds.

20 June 1986; accepted 9 October 1986

## Mapping Human Brain Monoamine Oxidase A and B with <sup>11</sup>C-Labeled Suicide Inactivators and PET

J. S. FOWLER, R. R. MACGREGOR, A. P. WOLF, C. D. ARNETT, S. L. DEWEY, D. SCHLYER, D. CHRISTMAN, J. LOGAN, M. SMITH, H. SACHS, S. M. AQUILONIUS, P. BJURLING, C. HALLDIN, P. HARTVIG, K. L. LEENDERS, H. LUNDQVIST, L. ORELAND, C.-G. STÅLNACKE, B. LÅNGSTRÖM

The regional distributions of monoamine oxidase (MAO) types A and B have been identified in human brain in vivo with intravenously injected <sup>11</sup>C-labeled suicide enzyme inactivators, clorgyline and L-deprenyl, and positron emission tomography. The rapid brain uptake and retention of radioactivity for both <sup>11</sup>C tracers indicated irreversible trapping. The anatomical distribution of <sup>11</sup>C paralleled the distribution of MAO A and MAO B in human brain in autopsy material. The corpus striatum, thalamus, and brainstem contained high MAO activity. The magnitudes of uptake of both [<sup>11</sup>C]clorgyline and L-[<sup>11</sup>C]deprenyl were markedly reduced in one subject treated with the antidepressant MAO inhibitor phenelzine. A comparison of the brain uptake and retention of the <sup>11</sup>C-labeled inactive (D-) and active (L-) enantiomers of deprenyl showed rapid clearance of the inactive enantiomer and retention of the active enantiomer within MAO B-rich brain structures, in agreement with the known stereoselectivity of MAO B for L-deprenyl. Prior treatment with unlabeled L-deprenyl prevented retention of L-[<sup>11</sup>C]deprenyl. Thus, suicide enzyme inactivators labeled with positron emitters can be used to quantitate the distribution and kinetic characteristics of MAO in human brain structures.

**M**ONOAMINE OXIDASE (MAO) (E.C. 1.4.3.4) is responsible for the oxidative deamination of endogenous neurotransmitter amines as well as amines from exogenous sources. It exists in two forms, MAO A and MAO B, which are identified by their inhibitor sensitivity and by their substrate selectivity (1). Both forms may be important for neurotransmitter regulation, and fluctuations in functional MAO

activity may be associated with human diseases such as Parkinson's disease, depression, and certain psychiatric disorders (2). A number of MAO inhibitors are used as antidepressant drugs (3); L-deprenyl, an inhibitor of MAO B, is used to treat Parkinson's disease (4), and brain MAO B plays a key role in 1-methyl-4-phenyl-1,2,3,6-tetrahydropyridine (MPTP)-induced parkinsonism (5). Speculation as to the relation of

MAO activity to human disease has been based on the measurement of platelet MAO activity or on the analysis of postmortem human brain samples. However, platelet MAO is only MAO B (6), and, although the platelet enzyme is probably a genetic marker for serotonergic mechanisms in the brain (7), direct attempts to correlate platelet and brain MAO B have failed (8). Furthermore, even the process of isolation of MAO from its native environment within a tissue for measurement in vitro may change some properties of the enzyme (9, 10).

A major milestone in the study of MAO has been the design and synthesis of the highly selective, mechanism-based inhibitors clorgyline (N-[3-(2,4-dichlorophenoxy)propyl]-N-methyl-2-propynylamine) (11) and L-deprenyl [(–)-N,α-dimethyl-N-2-propynylphenethylamine] (12), which irreversibly inhibit MAO A and MAO B, respectively, by binding covalently to the enzyme itself (13), a process frequently referred to as "suicide enzyme inactivation" (14).

We have explored the feasibility of using <sup>11</sup>C-labeled clorgyline and L-deprenyl for mapping functional MAO in brain directly and noninvasively by using the covalent bond formation between labeled inhibitor and enzyme to label the enzyme in a selective and irreversible manner. The regional

J. S. Fowler, R. R. MacGregor, A. P. Wolf, C. D. Arnett, S. L. Dewey, D. Schlyer, D. Christman, J. Logan, M. Smith, H. Sachs, Brookhaven National Laboratory, Upton, NY 11973.  
S. M. Aquilonius, P. Bjurling, C. Halldin, P. Hartvig, K. L. Leenders, H. Lundqvist, L. Orelan, C.-G. Stålnacke, B. Långström, University of Uppsala, Uppsala, Sweden.

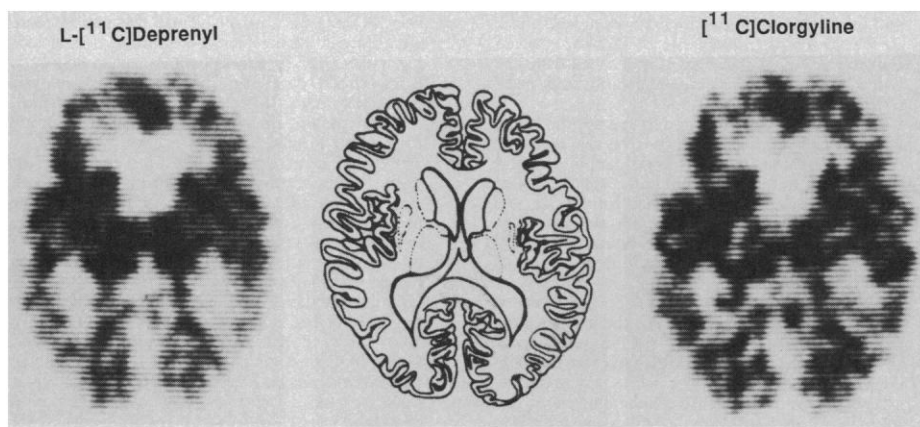


**Fig. 1.** PET scans at the level of corpus striatum and the thalamus after injection of [ $^{11}\text{C}$ ]clorgyline and L- $^{11}\text{C}$ ]deprenyl. Drawing of anatomical section corresponding to the brain level is shown (center).

distribution of the  $^{11}\text{C}$  label retained in tissue would reflect regional functional enzyme activity provided that (i) there is significant transport of the  $^{11}\text{C}$  inhibitor into the brain, (ii) the tracer is uniquely reactive with the enzyme subtype, and (iii) enzyme inactivation is rapid relative to formation of product (15). Carbon-11 is well suited for these studies. It has a 20.4-minute half-life and decays by positron emission, which results in the emission of two body-penetrating 511-keV photons. Simultaneous spatial and temporal measurement of the concentration of the tracer in the living brain (or other tissues) is possible with positron

emission tomography (PET) (16). Furthermore, we can do serial studies on the same day in the same subject at 2.5-hour intervals because (i) essentially all (>99.4%) of the  $^{11}\text{C}$  decays to nonradioactive  $^{11}\text{B}$  within 2.5 hours after its administration, and, therefore, residual radioactivity does not interfere with the next investigation; and (ii) the specific radioactivity of the  $^{11}\text{C}$  tracer is sufficiently high that only a small fraction of the total amount of MAO in the brain is irreversibly bound, which allows the  $^{11}\text{C}$ -labeled inhibitor to act as a true tracer (17). Initial studies demonstrating the specific uptake and covalent binding of [ $^{11}\text{C}$ ]clorgy-

line and L- $^{11}\text{C}$ ]deprenyl in mouse brain in vivo (18), and PET studies carried out in anesthetized baboons (19) before the initiation of human studies suggested this approach to the in vivo study of MAO activity in the human brain.

We report here the extension of the animal studies to an examination of the kinetic behavior and anatomical localization of [ $^{11}\text{C}$ ]clorgyline and L- $^{11}\text{C}$ ]deprenyl in human brain through the use of PET. We also present experimental evidence that the anatomical distribution and uptake of these tracers arise from attachment of labeled inhibitor to enzyme, which shows that the distribution of radioactivity in brain reflects functional MAO activity.

$^{11}\text{C}$ -Labeled clorgyline, D-deprenyl, and L-deprenyl were prepared by alkylation of the *N*-demethyl compounds with [ $^{11}\text{C}$ ]methyl iodide. Specific radioactivities were 175 to 445 mCi/ $\mu\text{mol}$  at the time of injection. Normal volunteers who had given informed consent (males, 26 to 86 years old) were injected intravenously with saline solutions of 8 to 18 mCi (13 to 31  $\mu\text{g}$ ) of L- $^{11}\text{C}$ ]deprenyl and then 2.5 hours later by 6 to 16 mCi (5 to 12  $\mu\text{g}$ ) of [ $^{11}\text{C}$ ]clorgyline. The order of injection was reversed in studies 3, 4, and 5 (Table 1). Arterialized venous blood samples obtained 0.17 to 110 minutes after injection of each tracer were centrifuged, and radioactivity was determined in aliquots of plasma. High-performance liquid chromatographic (HPLC) analyses of plasma samples taken at 1, 5, 10, and 30 minutes were performed to determine the time course of radiotracer metabolism. PET scanning (PETT VI) (20) began at the time of injection and continued for 90 minutes. An additional subject (male, 72 years old) who had been receiving a combination of the MAO inhibitor phenelzine (Nardil, 30 mg/day) and dextroamphetamine (Dexedrine, 2.5 mg/day) for 4 weeks as a treatment of depression underwent the same serial study with [ $^{11}\text{C}$ ]clorgyline and L- $^{11}\text{C}$ ]deprenyl. On the day of the study he received phenelzine 5 hours before injection of the first tracer, and the dextroamphetamine dose was withheld until after the study. Another normal volunteer (male, 68 years old) was injected with 3 mCi (10  $\mu\text{g}$ ) of D- $^{11}\text{C}$ ]deprenyl followed by 3 mCi (10  $\mu\text{g}$ ) of L- $^{11}\text{C}$ ]deprenyl with an intervening time of 2.5 hours. The PET scanning (Scanditronix type 384-3B) was similar to that described above. Three weeks after this series this same volunteer received a therapeutic dose (15 mg) of L-deprenyl, and the serial PET studies with labeled D- and L-deprenyl were performed 24 hours later.

The regional distribution of radioactivity at different times after injection was deter-

**Table 1.** Influx rate constants ( $K_i$ ) for four normal volunteers (studies 1 to 4) and one subject receiving phenelzine plus amphetamine for treatment of depression (study 5). Integrated plasma activity for the 30-minute time period after injection is also presented.

Study	Age	Region of interest	$K_i$ (milliliters of plasma per cubic centimeter of tissue per minute)*		$\int_0^{30 \text{ min}} C_p(t) dt$ (nCi ml $^{-1}$ min) $\dagger$	
			[ $^{11}\text{C}$ ] Clorgyline	L- $^{11}\text{C}$ ] Deprenyl	[ $^{11}\text{C}$ ] Clorgyline	L- $^{11}\text{C}$ ] Deprenyl
1	26	Striatum	0.21	0.44	2329	1818
		Thalamus	0.27	0.56		
		Cortex $\ddagger$	0.16	0.29		
		Brainstem	0.20	0.41		
2	34	Striatum		0.45	3206	2295
		Thalamus		0.51		
		Cortex $\ddagger$		0.28		
		Brainstem		0.41		
3	39	Striatum	0.18	0.71	3260	1018
		Thalamus	0.17	0.73		
		Cortex $\ddagger$	0.16	0.54		
		Brainstem	0.17	0.47		
4	86	Striatum	0.19	0.86	3611	1618
		Thalamus	0.22	0.86		
		Cortex $\ddagger$	0.12	0.53		
		Brainstem	0.15	0.64		
5	72	Striatum	0.07	0.27	3965	2776
		Thalamus	0.08	0.23		
		Cortex $\ddagger$	0.04	0.10		
		Brainstem	0.06	0.23		

\*Influx rate constants ( $K_i$ ) were calculated from the slope of the linear portion of the curve obtained by plotting  $C_t/C_p$  against  $\int_0^t C_p(t) dt/C_p$ . Radioactivity concentration data for experimental times of 15 to 90 minutes were used. Linearity was observed in all cases.  $\dagger$ Integrated plasma activity was obtained from values of the concentration of unchanged drug in the plasma [ $C_p(t)$ ] over the first 30 minutes after injection of the tracer. The values are corrected for the presence of  $^{11}\text{C}$ -labeled metabolites as determined by HPLC analysis. All values were normalized to a 10-mCi injection dose.  $\ddagger$ Samples taken from frontal, parietal, and occipital cortices.

mined for each tracer (21). The thalamus and striatum (caudate and putamen) were examined in the anatomical slice shown in Fig. 1. The cortex was selected from an averaged value from the frontal, parietal, and occipital cortices as these regions had similar radioactivity concentrations. The brainstem region (midbrain) was selected in the slice containing the cerebellar vermis and was located immediately anterior to this structure. Regional brain uptake values were calculated from the radioactivity per cubic centimeter corrected for decay divided by the total amount of  $^{11}\text{C}$ -labeled tracer injected per gram of body weight.

After the injection of radiolabeled clorgyline and deprenyl, radioactivity rapidly entered the brain and remained at a constant high level throughout the 90-minute PET study (Fig. 2). The magnitude of uptake for L- $^{11}\text{C}$ deprenyl surpassed that of  $^{11}\text{C}$ clorgyline by a factor of approximately 2 in thalamus, striatum, cortex, and brainstem. Plasma clearance of total radioactivity was rapid for both tracers, and the amount of unchanged tracer in plasma also declined from 95% to approximately 40% in the first 30 minutes after injection as determined by HPLC analysis. However, the analysis of radioactivity concentrations for equivalent doses (millicuries) of  $^{11}\text{C}$  tracer showed a significantly greater amount of  $^{11}\text{C}$ clorgyline than L- $^{11}\text{C}$ deprenyl in the plasma over a 30-minute time period for all subjects (Table 1). This lower blood clearance for  $^{11}\text{C}$ clorgyline was due to a slower clearance of total  $^{11}\text{C}$  from the plasma rather than a difference in the rate of appearance of  $^{11}\text{C}$ -labeled metabolites (which was similar for the two tracers). Hence more  $^{11}\text{C}$ clorgyline was actually available for influx into brain tissues. Graphical analysis (22) of the measured changes in radioactivity concentrations for brain and plasma showed irreversible trapping of tracer and allowed the calculation of a plasma-to-brain influx rate constant ( $K_i$ ) for each subject and each tracer (Table 1). The results of this graphical analysis and the observed rapid uptake and retention of each of these tracers are consistent with suicide enzyme inactivation.

After the administration of both  $^{11}\text{C}$ clorgyline and L- $^{11}\text{C}$ deprenyl, the distribution of radioactivity in different brain regions was highest in the thalamus, striatum, cortex, and brainstem (Fig. 1) and paralleled the areas of high MAO concentration determined by in vitro assay (23). For both tracers the radioactivity concentrations and the influx rate constants for striatum and thalamus were higher than those of cortex (Table 1). In addition, the  $K_i$ 's for L- $^{11}\text{C}$ deprenyl were consistently higher than those for  $^{11}\text{C}$ clorgyline, an observation

**Fig. 2.** Time course of uptake for  $^{11}\text{C}$ clorgyline (A) and L- $^{11}\text{C}$ deprenyl (B) in the corpus striatum (diamonds), thalamus (squares), and cerebral cortex (triangles) of a normal volunteer (86 years old). Uptake values were calculated from the nanocuries per cubic centimeter corrected for decay for a specific brain region divided by the radioactive dose given per gram of body weight.

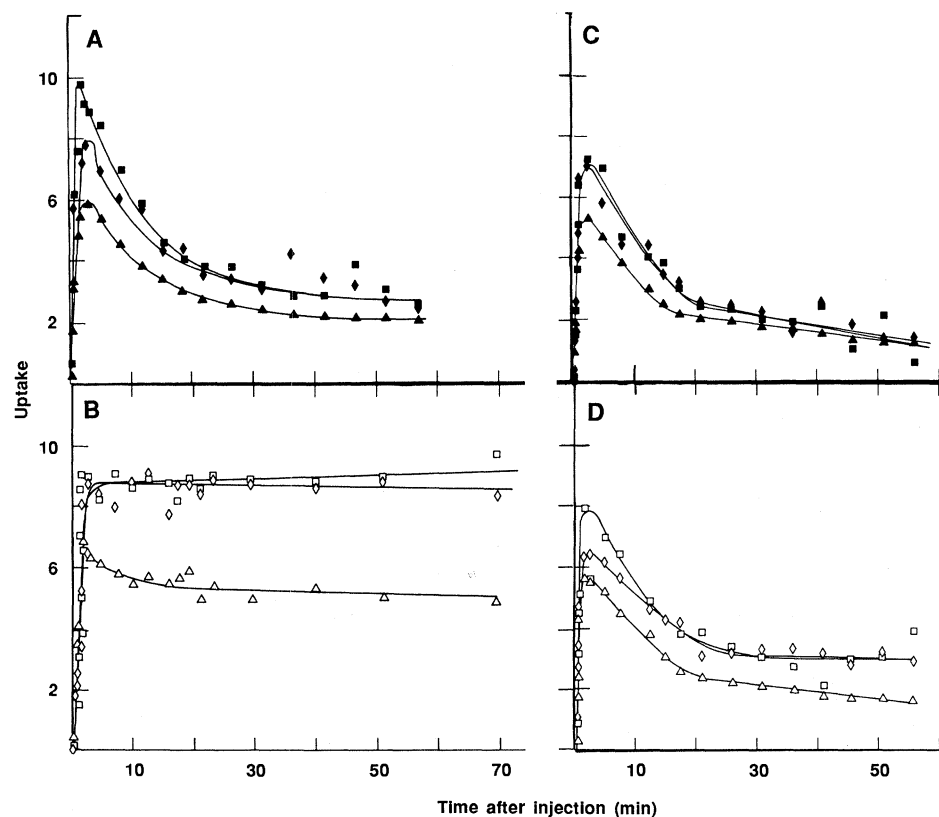
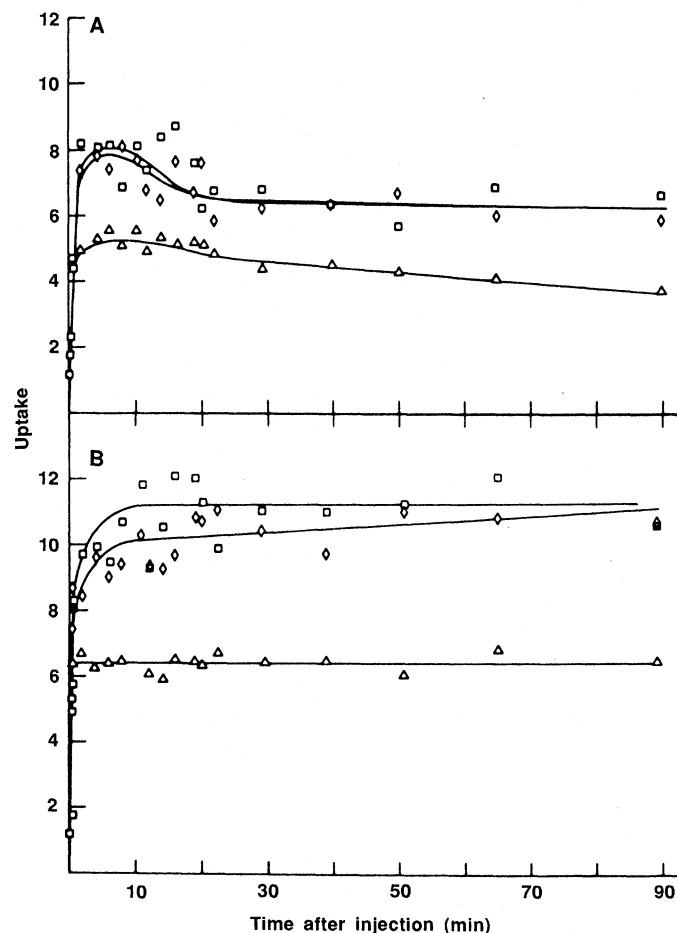


**Fig. 3.** A comparison of the time course of uptake of L- $^{11}\text{C}$ deprenyl (open symbols) and D- $^{11}\text{C}$ deprenyl (solid symbols) in striatum (diamonds), thalamus (squares), and cerebral cortex (triangles) before (A and B) and after (C and D) a 15-mg dose of unlabeled L-deprenyl (see legend to Fig. 2 for the definition of uptake).

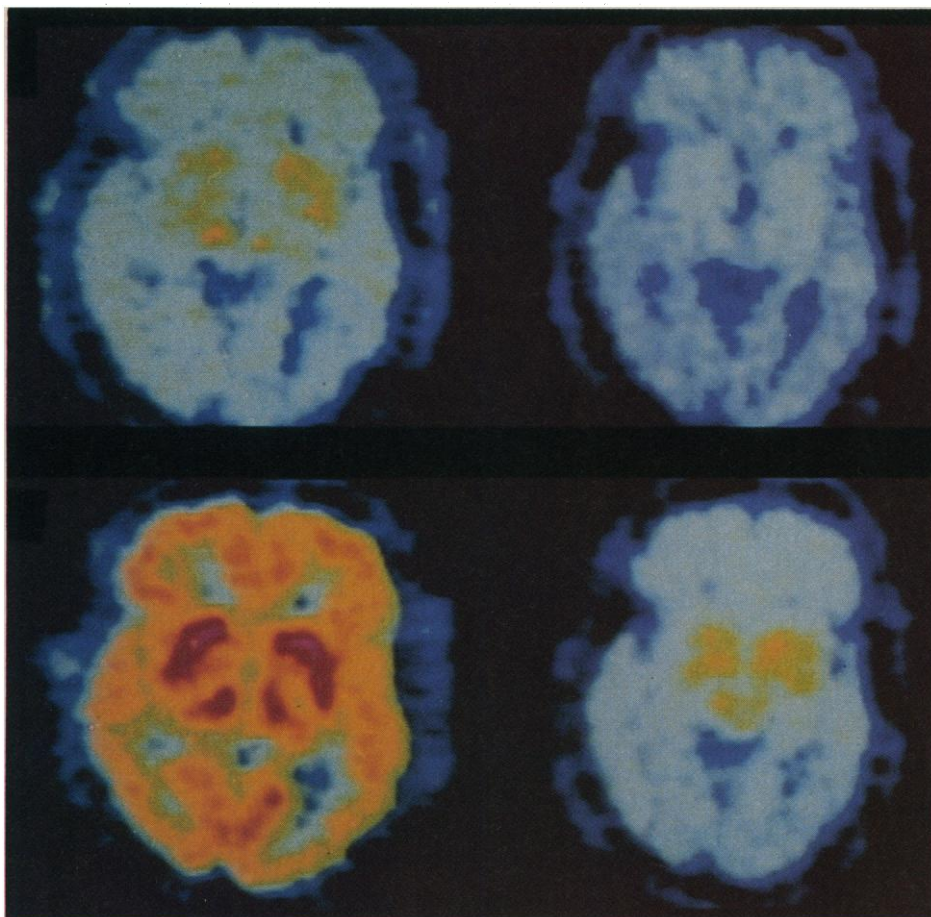


**Fig. 4.** PET images after administration of D-[ $^{11}\text{C}$ ]deprenyl (**top images**) and L-[ $^{11}\text{C}$ ]deprenyl (**bottom images**) in a normal volunteer before (left) and after (right) administration of 15 mg of L-deprenyl. The colors correspond to radioactivity concentration with red > yellow > blue. The PET slice is at the same level as Fig. 1.

that may reflect the higher concentration of MAO B than MAO A in human brain (24). In the four normal volunteers injected with both tracers, the  $K_i$ 's for [ $^{11}\text{C}$ ]clorgyline show less intersubject variability than those for L-[ $^{11}\text{C}$ ]deprenyl. Although the observed higher  $K_i$  for L-[ $^{11}\text{C}$ ]deprenyl could parallel the age of the volunteer and thus reflect the known increase in MAO B with age (24), the sample size reported in this study is too limited to permit a meaningful correlation.

In the one subject who was receiving the irreversible MAO inhibitor phenelzine in combination with amphetamine for treatment of chronic depression, we observed a significantly lower  $K_i$  for both tracers. This result provides further evidence supporting irreversible enzyme inhibition as the factor responsible for the regional uptake and retention of [ $^{11}\text{C}$ ]clorgyline and L-[ $^{11}\text{C}$ ]deprenyl. Phenelzine inhibits both MAO A and MAO B with a preference for MAO A (25) and would be predicted to influence the uptake of both tracers if MAO is responsible for the observed uptake and retention of the  $^{11}\text{C}$  tracers in normal volunteers.

Deprenyl, which contains an asymmetric

carbon atom, exists in two enantiomeric forms, D(S)-(+)-deprenyl and L(R)-(-)-deprenyl, which are synthesized from (S)-(+)-amphetamine and (R)-(-)-amphetamine, respectively. Because L(R)-(-)-deprenyl is 25 times as active with respect to MAO B inhibition as D(S)-(+)-deprenyl (26), serial PET studies with these two  $^{11}\text{C}$ -labeled enantiomers are a powerful tool in differentiating specific binding from nonspecific distribution because nonspecific distribution is generally not governed by stereoselective processes (27). A comparison of the time course of radioactivity distribution after injection of D-[ $^{11}\text{C}$ ]deprenyl with that after injection of L-[ $^{11}\text{C}$ ]deprenyl shows strikingly different kinetics. The appearance of D-[ $^{11}\text{C}$ ]deprenyl in the brain was initially similar to that of L-[ $^{11}\text{C}$ ]deprenyl, but the inactive D enantiomer cleared rapidly (Fig. 3). This observation is consistent with stereoselective labeling of MAO B, which determines the anatomical pattern of distribution as well as long-term retention of activity within brain tissue. The time course of radioactivity distribution with D-[ $^{11}\text{C}$ ]deprenyl (Fig. 3A) is similar to that observed

for L-[ $^{11}\text{C}$ ]deprenyl in a subject in whom brain MAO was inhibited by prior administration of a therapeutic dose of L-deprenyl (Fig. 3D). The selective uptake of L-[ $^{11}\text{C}$ ]deprenyl in striatum for a normal subject can be seen in Fig. 4 (bottom left image), which also shows PET images corresponding to the data for L-[ $^{11}\text{C}$ ]deprenyl and D-[ $^{11}\text{C}$ ]deprenyl plotted in Fig. 3.

The method we have used should prove useful in the examination of MAO A and MAO B activity in brain and thus provides a means of directly examining the two forms of MAO in intact living tissue (28). Since clorgyline and L-deprenyl have played a pivotal role in mechanistic studies of the properties of MAO A and MAO B (1) and are used as investigational drugs in the therapy of depression (29), and since L-deprenyl is currently used as an adjunct to L-dopa therapy of Parkinson's disease (30), the extensive base of knowledge resulting from their use is a valuable resource for future studies with PET and the  $^{11}\text{C}$ -labeled tracers. Furthermore, because these drugs are relatively nontoxic at doses sufficient to inhibit significant amounts of the enzyme (29), it may be possible to use in vivo titration to directly determine MAO concentration in living human brain, as has been done with autopsy material (24), and to correlate these measurements with clinical state in individuals afflicted with a variety of psychopathologies (7). Current studies are under way to use PET and L-[ $^{11}\text{C}$ ]deprenyl to measure the rate of recovery (synthesis) of MAO B after a single therapeutic dose of L-deprenyl (19)—a new approach to the measurement of the synthesis of a specific protein in vivo and a possible strategy for probing mitochondrial viability.

Although the study of brain MAO activity with this technique would obviously be of high priority because of its implication in neurological and psychiatric disorders, in principle MAO activity in other parts of the body could also be mapped with  $^{11}\text{C}$  tracers and high-resolution, large field of view PET, provided that experiments validating the mechanism of uptake and retention of tracers in organs other than brain were carried out. In addition, the rapidly increasing number of highly selective suicide enzyme inactivators suggests that methods for directly probing other enzymes in human brain and other tissues can be developed. This general approach, although most easily accomplished with positron-emitting labeled compounds and PET, would also be applicable to radiotracers labeled with  $\gamma$ -emitting isotopes through the use of single photon-emission computed tomography (SPECT), provided that these radiotracers displayed appropriate behavior in vivo.

REFERENCES AND NOTES

1. C. J. Fowler, L. Oreland, B. A. Callingham, *J. Pharm. Pharmacol.* **33**, 341 (1981).
2. K. F. Tipton, P. Dostert, M. Strolin Benedetti, Eds., *Monoamine Oxidase and Disease* (Academic Press, New York, 1984).
3. M. B. H. Youdim and J. P. M. Finberg, *Mod. Probl. Pharmacopsychiatry* **19**, 63 (1983).
4. M. DaPrada, H. H. Keller, L. Pieri, R. Kettler, W. E. Haefely, *Experientia* **40**, 1165 (1984).
5. J. W. Langston, I. Irwin, E. B. Langston, L. S. Forno, *Science* **225**, 1480 (1984).
6. M. Sandler, M. Reveley, V. Glover, *J. Clin. Pathol.* **34**, 292 (1981).
7. L. Oreland, L. V. Knorrning, D. Schalling, *Proceedings of the IUPHAR* [International Union of Pharmacology] *Ninth International Congress of Pharmacology* (Macmillan, London, 1984), vol. 2, pp. 193-202.
8. B. Winblad, C.-G. Gottfries, L. Oreland, A. Wiberg, *Med. Biol.* **57**, 129 (1979); W. F. Young, E. R. Laws, F. W. Sharbrough, R. M. Weinsilboum, *Arch. Gen. Psychiatry* **43**, 604 (1986).
9. S. Urwyler and J.-P. von Wartburg, *Biochem. Pharmacol.* **29**, 3067 (1980).
10. L. B. Pearce and J. A. Roth, *Biochemistry* **24**, 1821 (1985).
11. J. P. Johnston, *Biochem. Pharmacol.* **17**, 1285 (1968).
12. J. Knoll and K. Magyar, *Adv. Biochem. Psychopharmacol.* **5**, 393 (1972).
13. R. R. Rando, *Pharmacol. Rev.* **36**, 111 (1984).
14. R. H. Abeles and A. L. Maycock, *Acc. Chem. Res.* **9**, 313 (1976).
15. S. G. Waley, *Biochem. J.* **227**, 843 (1985).
16. M. E. Phelps, J. C. Mazziotta, H. Schelbert, Eds., *Positron Computed Tomography* (Raven, New York, 1985).
17. Typical specific activities obtained for  $^{11}\text{C}$  tracers are in the range of 175 to 445 mCi/ $\mu\text{mol}$  at time of injection. Thus a 10-mCi injection corresponds to 0.02 to 0.06  $\mu\text{mol}$  of the inhibitor. By using 5 pmol of MAO B per milligram of protein as an estimate of brain MAO B concentration [L. Oreland and C. J. Fowler, in *Monoamine Oxidase: Structure, Function and Altered Functions*, T. Singer, R. V. Korff, D. Murphy, Eds. (Academic Press, New York, 1979), pp. 389-396], the total MAO content of the brain (100 g of protein) can be estimated to be about 0.5  $\mu\text{mol}$ . If 5% of the injected dose is taken up by brain tissue, then 0.001 to 0.003  $\mu\text{mol}$  of labeled inhibitor is available for irreversible enzyme inhibition. If there is a stoichiometric inhibition of enzyme by labeled inhibitor, then <1% of the total brain MAO would be irreversibly inhibited in a typical PET study.
18. R. R. MacGregor *et al.*, *Biochem. Pharmacol.* **34**, 3207 (1985).
19. C. D. Arnett *et al.*, *J. Nucl. Med.* **27**, 982 (1986).
20. M. TerPogossian, D. C. Ficke, J. T. Hood, M. Yamamoto, N. A. Mullani, *J. Comp. Assist. Tomography* **6**, 125 (1982).
21. The two positron emission tomographs used in these studies had an in-plane resolution of 8 to 9 mm and an axial resolution of 14 mm. The examination of regional distribution of radioactivity after injection of [ $^{11}\text{C}$ ]clorgyline and L-[ $^{11}\text{C}$ ]deprenyl was limited to relatively large brain structures (>2  $\text{cm}^3$ ) because of the resolution of the instruments.
22. C. S. Patlak, R. G. Blasberg, J. D. Fenstermacher, *J. Cereb. Blood Flow Metab.* **3**, 1 (1983).
23. L. Oreland, Y. Arai, A. Stenström, C. J. Fowler, *Mod. Probl. Pharmacopsychiatry* **19**, 246 (1983).
24. C. J. Fowler, L. Oreland, J. Marcusson, B. Winblad, *Naunyn Schmiedeberg's Arch. Pharmacol.* **311**, 263 (1980).
25. H. H. Miller, P. A. Shore, D. E. Clarke, *Biochem. Pharmacol.* **29**, 1347 (1980).
26. J. B. Robinson, *ibid.* **34**, 4105 (1985).
27. T. Walle and U. K. Walle, *Trends Pharmacol. Sci.* **7**, 155 (1986).
28. Others have shown interest in the use of PET to evaluate MAO activity by the use of either a labeled inhibitor [K. Ishiwata *et al.*, *J. Nucl. Med.* **26**, 630 (1985)] or a labeled substrate [O. Inoue, T. Tomimaga, T. Yamasaki, H. Kinemuchi, *J. Neurochem.* **44**, 210 (1985)].
29. D. L. Murphy *et al.*, *Mod. Probl. Pharmacopsychiatry* **19**, 287 (1983).
30. W. Birkmayer *et al.*, *J. Neural Transm.* **64**, 113 (1985).
31. This research was carried out in part at Brookhaven National Laboratory (BNL) under contract DE-AC02-76CH00016 with the U.S. Department of Energy and supported by its Office of Health and Environmental Research and by the National Institutes of Health, grant NS-15638; it was also carried out in part at the University of Uppsala with the support of the Swedish Medical Research Council and the Swedish Natural Science Research Council, grant KKK-3464. We thank R. Hitzman for helpful discussions and K. Karlstrom, R. Gard, P. King, A. Tesoro, and E. Jellert for their assistance in performing these studies; R. Carciello, C. Barrett, and D. Warner for cyclotron operations; P. Malmberg for tandem accelerator operations; and BNL Medical Department personnel N. Netusil, J. Vail, T. Johnson, and H. Ulyat for patient preparation and supervision.

11 August 1986; accepted 7 November 1986